



Vertical Fine-Scale Distribution of *Calanus sinicus* in the Yellow Sea Cold Water Mass During the Over-Summering Process

Jun Pan^{1,2,3†}, Fangping Cheng^{4,5†}, Fei Yu^{1,2,3,6,7*}, Yongqiang Shi^{8*}, Fan Sun^{1,2,6}, Guangcheng Si^{1,2,3,6}, Chuanjie Wei^{1,2,3}, Xinyuan Diao^{1,2,3} and Yongfang Zhao^{1,3,9}

¹ Institute of Oceanology, Chinese Academy of Sciences (CAS), Qingdao, China, ² University of Chinese Academy of Sciences, Beijing, China, ³ Center for Ocean Mega-Science, Chinese Academy of Sciences (CAS), Qingdao, China, ⁴ CAS Key Laboratory of Marine Ecology and Environmental Sciences, Institute of Oceanology, Chinese Academy of Sciences (CAS), Qingdao, China, ⁵ Key Laboratory of Marine Ecosystem Dynamics and Second Institute of Oceanography, Ministry of Natural Resources, Hangzhou, China, ⁶ CAS Key Laboratory of Ocean Circulation and Waves, Chinese Academy of Sciences (CAS), Qingdao, China, ⁷ Marine Dynamic Process and Climate Function Laboratory, Pilot National Laboratory for Marine Science and Technology (Qingdao), Qingdao, China, ⁸ Yellow Sea Fisheries Research Institute, Chinese Academy of Fishery Sciences, Qingdao, China, ⁹ The Jiaozhou Bay Marine Ecosystem Research Station, Chinese Academy of Sciences (CAS), Qingdao, China

OPEN ACCESS

Edited by:

Alberto Basset,
University of Salento, Italy

Reviewed by:

Vladimir G. Dvoretzky,
Murmansk Marine Biological Institute,
Russia
Wei-Dong Zhai,
Shandong University, China

*Correspondence:

Fei Yu
yuf@qdio.ac.cn
Yongqiang Shi
shiyq@ysfri.ac.cn

† These authors have contributed
equally to this work

Specialty section:

This article was submitted to
Marine Ecosystem Ecology,
a section of the journal
Frontiers in Marine Science

Received: 19 December 2020

Accepted: 06 September 2021

Published: 27 September 2021

Citation:

Pan J, Cheng F, Yu F, Shi Y, Sun F,
Si G, Wei C, Diao X and Zhao Y
(2021) Vertical Fine-Scale Distribution
of *Calanus sinicus* in the Yellow Sea
Cold Water Mass During
the Over-Summering Process.
Front. Mar. Sci. 8:644043.
doi: 10.3389/fmars.2021.644043

Calanus sinicus, a temperate copepod with a lethal temperature $>27^{\circ}\text{C}$, is one of the key species in Chinese coastal marine ecosystems. The *C. sinicus* population increases in spring and declines in early summer annually due to increasing water temperature. Numerous *C. sinicus* individuals then congregate in the Yellow Sea Cold Water Mass (YSCWM) and remain under the thermocline from early summer to early autumn. Development and reproduction is halted in this cold and foodless bottom water and they avoid ascending to the hot surface water, which is regarded as an over-summering strategy. Based on discrete water sampling approaches, previous studies demonstrated that higher chlorophyll a (Chl a) levels appeared in the mixed hot surface water layer; however, the subsurface chlorophyll a maximum layer (SCML) has seldom been described. In the present study, various probes and a visual plankton recorder (VPR) were used to determine the fine vertical distributions of environmental factors and *C. sinicus*. VPR observations showed the ecological responses in fine scale and indicated that few *C. sinicus* individuals ascend at night, the main population preferred to remain below the SCML all day long. The results demonstrated that a constant thin SCML existed in the YSCWM area, and that the SCML location coincided with or was beneath the thermocline and halocline layers, where the temperature was suitable for *C. sinicus*. The relationship between abundance and Chl a, showed the diel vertical migration trend of *C. sinicus* to feed at night in the YSCWM area. In addition to temperature as a main influencing factor, dissolved oxygen concentrations and column depth were also influencing factors. Therefore, in addition to avoiding high surface temperature, energy supplement may be an important driving force confining the diel vertical migration of *C. sinicus* in the Yellow Sea in summer.

Keywords: copepod, *Calanus sinicus*, Yellow Sea Cold Water Mass, diel vertical migration, subsurface chlorophyll a maximum layer

INTRODUCTION

Calanus sinicus is a warm-temperate copepod species widely distributed in the shelf ecosystems of the Northwest Pacific Ocean (Chen, 1964; Li et al., 2016), and plays an important role in the marine food web (Uye, 2000; Sun et al., 2010). It is a key species in China's marine pelagic ecosystems, contributing 73–99% of the biomass of the large copepod functional group all year round in the Yellow Sea (Sun et al., 2010; Kim and Kang, 2018). The *C. sinicus* population usually disappears during summer in most parts of southern China seas due to increased water temperature (Li et al., 2016). However, the population remains in the Yellow Sea all year round (Chen, 1964; Li et al., 2016). Numerous *C. sinicus* individuals reside in the Yellow Sea Cold Water Mass (YSCWM) to survive through the hot summer, which is regarded as an over-summering strategy (Zhang et al., 2005). The fifth copepodite stage (C5) and female individuals dominate the population during the over-summering process, exhibiting low ingestion and metabolic rates, suspended development, confined diel vertical migration (DVM), a well-developed oil sac, and a low RNA:DNA ratio (Li et al., 2004; Zhou and Sun, 2016; Wang et al., 2017). In autumn, *C. sinicus* in the YSCWM serve as the parental individuals for population development and can be transported southward by monsoon-driven currents (Hwang and Wong, 2005; Yin et al., 2011). These physiological and ecological phenomena are similar to the over-wintering strategy of the dormant copepod species *Calanus finmarchicus* in the North Atlantic Ocean (Jónasdóttir, 2010).

The *C. sinicus* population dynamics has mainly been examined using water samplers or nets in the Yellow Sea (Li et al., 2004; Zhang et al., 2005). However, these traditional approaches might obscure the behavioral details and ecological responses in fine scale, such as vertical migration, feeding rhythm, predator avoidance, and the vertical distribution pattern of *C. sinicus* (Pan et al., 2018). The refined vertical distribution of *C. sinicus* in the YSCWM with corresponding environmental factors needs to be studied during the over-summering period, to enhance our understanding of relationships between the ecological strategies of *C. sinicus* and environmental elements (Ross, 2014; Stanley et al., 2017), and to improve zooplankton models (Everett et al., 2017).

The Visual Plankton Recorder (VPR) has been used to examine real-time abundance and distribution of zooplankton individuals for over two decades (Davis et al., 1992; Ashjian et al., 2001). By imaging a given water volume and various fitting sensors, the VPR can continuously provide images of plankton species and simultaneous environmental elements, such as temperature, salinity, nitrate, and fluorescent chlorophyll a (Chl a) concentration (Benfield et al., 1996; Davis et al., 2005). Previous studies have shown that the VPR can provide comparable information to net samples on plankton vertical and horizontal distributions with accurate species components, and moreover fine scale distribution information (Broughton and Lough, 2006; Takahashi et al., 2015).

The vertical position of copepod individuals might be a tradeoff of many factors, such as temperature, light intensity, food concentration, and predator abundance, producing different

fitness that appears as mortality, growth rate and birth rate. The VPR can help to illustrate the copepod vertical distribution, improve comprehension of the profound consequences of vertical distribution and shed light on the behavioral feedback to environmental factors (Bo et al., 2006; Sainmont et al., 2014). In this study, we used the VPR to 1) describe the horizontal and vertical distributions of *C. sinicus*, and 2) represent the transformation of hydrographical conditions across the YSCWM, to determine the influences of the thermocline and fluorescence on the vertical and horizontal distributions of *C. sinicus*.

MATERIALS AND METHODS

Sampling Area and Time in the Yellow Sea

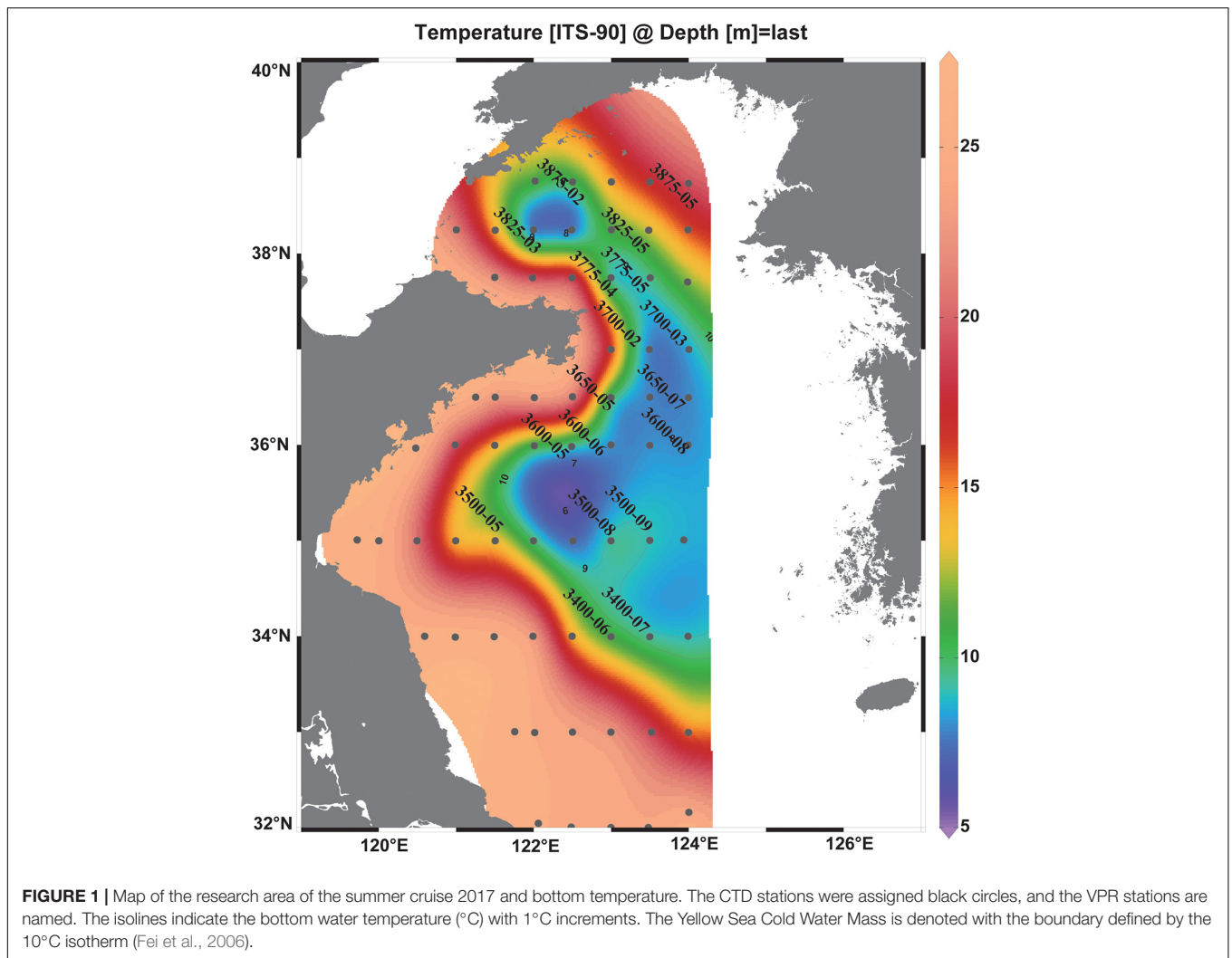
The Yellow Sea is a shallow and semi-closed marginal sea between the Chinese mainland and Korean Peninsula. The YSCWM is a seasonal water mass that is characterized by low temperature (<9°C) and high salinity (>32.5), occupying the third deepest part of the Yellow Sea in summer (Wang et al., 2003; Park et al., 2011). The formation of the YSCWM in summer has a significant impact on hydrographic features, biogeochemical cycles, marine planktonic biomass, and fishery resources in the Yellow Sea (Huo et al., 2012; Su et al., 2013).

The present investigation was conducted during a cruise in the Yellow Sea from 25 August to 7 September 2017 (**Figure 1**). A zooplankton net (mesh size: 505 mm) was hauled vertically from a depth of 2–4 m above the bottom to the surface at a speed of 1 m s⁻¹. Zooplankton samples were collected by the vertical net, which were then preserved in 5% formalin seawater solution after collection, identification and counting for morphological verification in the laboratory by ZooScan.

Temperature and salinity were recorded by a CTD instrument (Seabird 911) at all stations. The vertical profiles of turbidity, fluorescence, concentration of dissolved oxygen (DO), and nitrate were generated in each station simultaneously by equipment such as FLNTU (Wetlabs ECO Puck), DO (SBE-43), and Submersible Ultraviolet Nitrate Analyzer (SUNA) sensors. The CTD and additional sensors were calibrated before the cruise.

Survey of Visual Plankton Recorder and Environmental Elements Using Sensors

We employed the VPR for vertical tows from the bottom to the surface with the running speed at approximately 0.5–1 m s⁻¹ (Norrbín et al., 2009), and the sampling stations are shown in **Table 1**. The VPR used in the study consisted of two pressure cases, one which contained a Uniq UC-1830CL camera equipped with lenses that used four stepper motors (S0–S3) for accurate and repeatable positioning of the camera-lens extension, and the other contained a high-powered strobe in a ring configuration. The camera could generate compressed pictures with 1 megapixel resolution (1,024 × 1,024), and 10-bit color depth in the frame rate of around 15 s⁻¹ via an RS232 interface.



The imaged volume was calibrated before the survey using calibration files and calibration software (VPR_Cal) (Sainmont et al., 2014). Each VPR tow produced a file consisting of compressed images that were captured and recorded by the embedded computer stack. The pictures were obtained by the camera using the highest magnification with a field view of 42 × 42 mm (Ashjian et al., 2001; Sainmont et al., 2014). The ancillary CTD data were transmitted to a processing computer by two methods (USB adapter or Ethernet cable) after every VPR tow.

Data Analysis

The images were as determined for the gradient in grayscale and segmented at a user-selected brightness threshold (Davis et al., 1992; Ross, 2014). Regions of Interest (ROIs) were named by sampling time in milliseconds and stored in a special data directory structure. They were then time-stamped for subsequent spatial mapping (time in milliseconds within the day) and sampling depth via the time stamp using Mathworks (MATLAB software, 2015a), in order to allow them to be merged with the

data from the CTD which were written in separate data files (Davis et al., 2005; Gislason et al., 2016).

Regions of interests were sorted automatically into different taxa using classifiers after training with a set of images of taxa assigned by morphological identifying specialists. All classified ROIs were subsequently checked manually to confirm classification and counted (Hu and Davis, 2006; Gislason et al., 2016). The hydrographic parameters could also be related to the ROIs by time stamping. Images of different taxa were listed by observation times and binned into 1s bins of sensor data, and then counted. The image volume and counts of manually sorted images were used to calculate abundance and then plotted with vertical profiles of physical parameters (Davis et al., 2005; Sainmont et al., 2014; Gislason et al., 2016).

The formula used to calculate abundance was as follows:

$$Abu = \frac{N_{ind}}{N_{frame} \times Volume} \times 10^3 \quad (1)$$

Where, Abu is the number of individuals per cubic meter, N_{ind} is the number of individuals observed in a second, N_{frame} is the

number of frames per second, and Volume is the image volume of a single frame (e.g., S3 setting, the volume is 300 ml).

For S3 stepper, the camera was focused such that the field of view of each image was 42 mm × 42 mm, the lens was adjusted to give a field of view of 1.7 cm and the calibrated image volume was 300 ml (Davis et al., 2005). The horizontal distribution of *C. sinicus* was related to water depth, number of detected individuals e.g. the cross section is $w = 42$ mm, $l = 170$ mm, $h = \text{depth (m)}$, the volume is $w \times l \times h$ (m³); and the horizontal abundance is the number of individuals detected/volume (ind/m³).

As *C. sinicus* is the dominant species in the Yellow Sea with a main body size of 2.4–3.5 mm (Chen, 1964), VPR S3 setting was chosen as the main stepper in this study. The range of zooplankton length that appeared in the obtained images was generally 1.8–16 mm. We did not discriminate the developmental stages of *C. sinicus* due to some ambiguous images. However, they did not hamper identification of *C. sinicus*, as it highly dominated at most stations according to the net samples and its obvious exterior helped identification. Based on the Savitzky-Golay method, the profiles of *C. sinicus* abundance are shown using MATLAB (R2015a). According to the DIVA gridding method, vertical profiles of temperature, salinity, fluorescence and nitrate were visualized using Ocean Data View software version (4.7.6) (Schlitzer, 2002). The depth of the subsurface Chl a maximum layer (SCML) was determined by the downward profile of fluorescence.

RESULTS

Environmental Conditions

All VPR stations were under highly stratified conditions, and temperature, salinity, and concentrations of dissolved oxygen (DO) generally exhibited steep changes between 10 and 40 m depth (Figure 2). The thickness of the thermocline (>0.5°C change in 1 m depth interval) ranged from 5 to 20 m (Figure 2). The boundary of the YSCWM was defined by the 10°C bottom isotherm (Fei et al., 2006; Figure 1). Most of the VPR stations in our survey (13 stations in all) were inside the YSCWM, and three stations (3400-06, 3825-05, and 3875-02) were outside and located at the edge of the YSCWM frontal area (bottom temperatures were <11.4°C). In addition, two stations (3500-05 and 3875-05) were located outside the YSCWM with bottom temperatures > 14.1°C (Figures 1, 2). The spatial coverage of the YSCWM was observed from 122°E to 124°E and from 34°N to 38°N in this study.

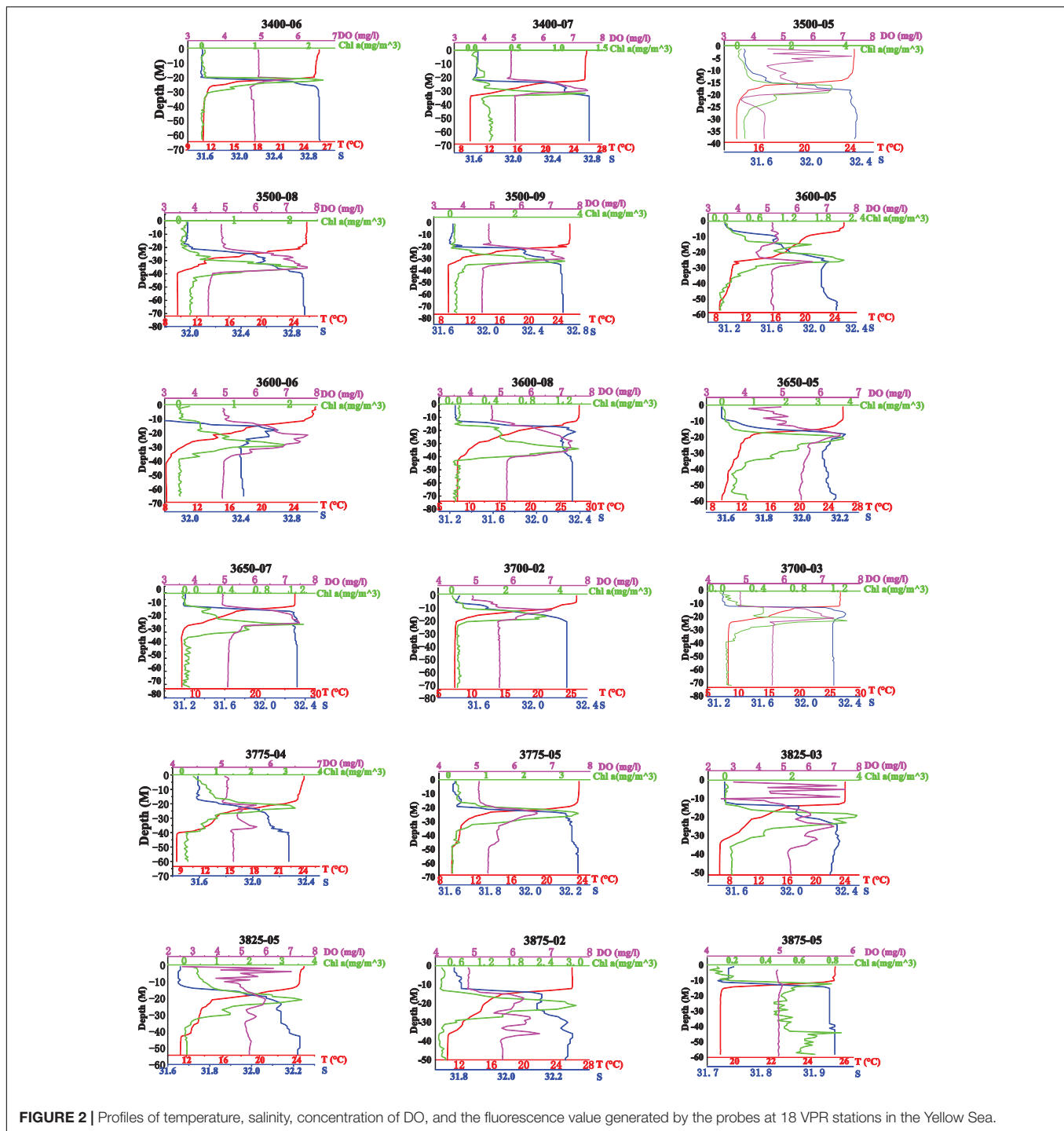
The range of salinity was 28.5–32.9, the salinity coverage in the YSCWM was more than 32. The salinity ranged from 31.16 to 32.93 among the 18 VPR stations, generally showing inverse changes compared with the temperature, and the haloclines mirrored the thermoclines at most stations (Figure 2). Above the thermocline, there was a mixed layer of warm water (>23°C) with salinity < 31.9. The bottom water showed relatively high salinity (>32) and low

TABLE 1 | Time and depths of VPR stations used during August to September, 2017.

Cast	Location	Data (Day/Month/Year)	Local time	Sampling Depth (m)	Bottom Depth (m)
3400-06	34°N, 123°E	07/September/2017	15:00	0–65	67
3400-07	34°N, 123.5°E	07/September/2017	19:00	0–67	69
3500-05	35°N, 121.5°E	02/September/2017	10:00	0–35	39
3500-08	35°N, 123°E	02/September/2017	1:00	0–68	72
3500-09	35°N, 123.5°E	01/September/2017	23:00	0–72	77
3600-05	36°N, 122.5°E	25/August/2017	7:00	0–55	59
3600-06	36°N, 123°E	25/August/2017	11:00	0–67	70
3600-08	36°N, 124°E	25/August/2017	17:00	0–75	77
3650-05	36.5°N, 123°E	26/August/2017	2:00	0–59	61
3650-07	36.5°N, 124°E	25/August/2017	21:00	0–74	76
3700-02	37°N, 123.5°E	27/August/2017	10:00	0–66	72
3700-03	37°N, 124°E	27/August/2017	13:00	0–74	75
3775-04	37.75°N, 123°E	31/August/2017	17:00	0–57	63
3775-05	37.75°N, 123.5°E	01/September/2017	5:00	0–69	70
3825-03	38.25°N, 122°E	31/August/2017	7:00	0–50	54
3825-05	38.25°N, 123°E	31/August/2017	18:00	0–54	55
3875-02	38.75°N, 122.5°E	28/August/2017	6:00	0–48	52
3875-05	38.75°N, 124°E	27/August/2017	22:00	0–55	60

temperature, ranging from 6.6°C (38.25°N, 122°E) to 14.2°C (35°N, 121.5°E) with the exception of station 3875-05 (bottom temperature 19.2°C, bottom salinity 31.94). The maximum temperature difference between the surface and bottom layers was up to 20.0°C in the center of the YSCWM (Figure 2). The concentration of DO in the water column of the stations assessed using a calibrated sensor varied from 2.60 to 7.66 mg. L⁻¹. In addition, the concentration of DO increased from the surface layer to the thermocline and was always higher near the SCML, then decreased with increased depth (Figures 2, 3).

A pronounced SCML formed around 15–30 m inside or below the thermocline at most stations except station 3875-05 (Figure 3). The highest fluorescence values of the SCML at all stations were from 1.3 to 3.65 mg. m⁻³ according to the fluorescence probe. The SCML may contribute substantial phytoplankton biomass in the water column. Our results also showed that the depth of the SCML was shallower (about 20 m) in the middle of the YSCWM region and the northern Yellow Sea, and was deeper (30 to 40 m) in the eastern part of the YSCWM region (Figure 3). We statistically analyzed the mean values and standard deviation of depth, Chl a, temperature, salinity and oxygen which are shown in Table 2. Pearson correlation analysis was performed to examine the relationships between *C. sinicus* abundance and environmental factors (Table 3).



Distribution of *Calanus sinicus* in the Yellow Sea

Calanus sinicus was detected by the VPR at all 18 stations and verified using the monograph ‘Atlas of Common Zooplankton of Chinese Coastal Seas’ (Sun et al., 2016). *C. sinicus* abundance was high at temperatures ranging from 6 to 10°C in summer. The abundance of *C. sinicus* was high at the optimal salinity from 32 to 32.9 during summer. In general, the results from most

stations indicated that the majority of the *C. sinicus* population remained below the thermocline and the SCML all day long and rarely appeared above the thermocline (Figures 2, 3). The only exception was found at station 3825-05, located between Yantai and Dalian. Only a few *C. sinicus* individuals were detected in the SCML by the VPR at stations 3600-05, 3650-05, 3775-04, 3775-05, 3825-03, 3825-05, and 3875-02 (Figure 3). However, at some night stations, such as 3400-07, 3500-08, 3500-09, 3600-08, and

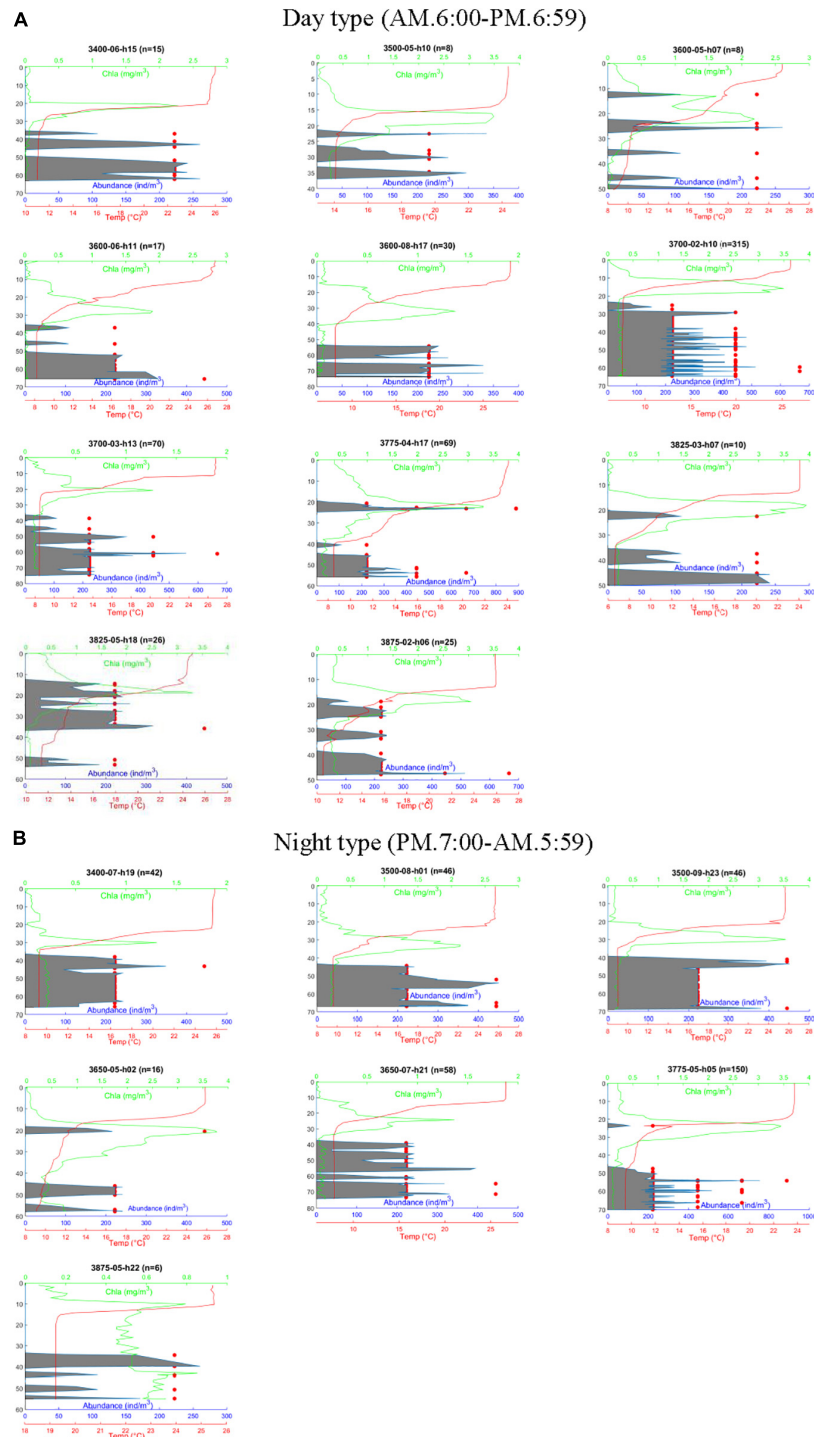


FIGURE 3 | Vertical profiles of *Calanus sinicus* abundance, chlorophyll concentration, and temperature in the Yellow Sea. *C. sinicus* was captured using the VPR and numerated by morphometrics, while the other factors were surveyed using probes. Red dots represent the abundance of *C. sinicus* at a specific depth; gray areas represent the moving average of *C. sinicus* abundance based on the Savitzky-Golay method using MATLAB. **(A)** Day type. **(B)** Night type; n: total number of individuals captured by the VPR; h: survey time (24 h).

3650-07, they were not detected in or above the SCML and the thermocline (**Figure 3**). The peak of *C. sinicus* abundance at each station ranged from 222.2 to 888.9 ind/m³ (**Figure 3**). The highest

abundance of *C. sinicus* appeared at station 3775-04 (in the SCML) and station 3775-05 (in the layer below the thermocline). Both stations are located in the northern Yellow Sea.

We also used a plankton net (505 μm) to collect samples at 17 stations, but not at station 3400-07, as the net sample was unavailable. We calculated the abundance of *C. sinicus* at each station to show the horizontal distribution. The VPR range of abundance was 15.3–668.4 ind/ m^3 . To validate the copepod abundance results obtained by ZooScan, the net sample results are also shown. A similar pattern was revealed by both the VPR and the plankton net (Figure 4). The plankton net results showed that the area with high abundance was similar to the area calculated by the VPR, and the order of magnitude was the same, which proved that the VPR had high sampling accuracy. Net sample results usually reflect the overall distribution of *C. sinicus* at each station. Shi et al. (2019) showed the distribution results using a steel sampler at different depths (0, 5, 10, 20, 35, 50, 75, and 2–5 m from the bottom) in order to improve the vertical distribution of *C. sinicus* abundance.

DISCUSSION

Potential Roles of Chlorophyll A, Subsurface Chlorophyll A Maximum Layer, and Dissolved Oxygen

The survey stations were located in the YSCWM-influenced area, where the hydrodynamic environment is relatively stable in summer (Fei et al., 2006; Xia et al., 2006). Strong stratification, which suspended physical mixing of the upper seawater layer and the layer below the thermocline, led to limited nutrients for phytoplankton growth and generated low fluorescence in the surface waters of the YSCWM area (Wei et al., 2016). The rhythm of both the nutricline and SCML depths were coincident with the pycnocline depth due to stratification in summer, which has been reported by in situ studies in the Yellow Sea (Zhou and Sun, 2016). The SCML was found to be only several meters thick in the YSCWM area in summer using a submersible fluorometer probe in situ (Li et al., 2011). Consequently, few studies have described the detailed vertical distribution pattern of chlorophyll fluorescence values and the thin phytoplankton layer. Photosynthetic pigment analysis indicated a steep peak of fluorescence which coincided with or beneath the depth of the SCML (Fu et al., 2009). The SCML has been attributed to the contribution of brown algae and green algae, and is controlled by the mechanism of vertical nutrients transport and the depth of the pycnocline. The present study showed that the SCML appeared at 17 of 18 stations (Figure 3). The profiles of Chl a were closely related to those of nitrate, which was in accordance with the results of previous studies (Gong et al., 2017). In the present study, the fluorescence probe provided the fine scale vertical profiles of primary production and reliable food concentration data in the Yellow Sea.

Sun et al. (2020) showed that decreasing DO had potential negative effects on early recruitment of *C. sinicus* in the northern Yellow Sea, China. However, low DO (4–6 mg/L) may not affect the survival rate of *C. sinicus* (Wang et al., 2013). In the present study, the abundance of detected *C. sinicus* and the environmental factors at a typical YSCWM station (3500-09) were used in the Pearson correlation analysis (Table 3).

TABLE 2 | Average values of environmental factors at 18 stations by VPR and CTD.

Factor	Mean values	Standard deviation	Median
Temperature ($^{\circ}\text{C}$)	9.162	2.347	8.526
Salinity	32.356	0.229	32.264
Depth (m)	53.002	12.619	55.386
Oxygen (mg/L)	5.31	0.402	5.303
Chl a (mg/ m^3)	0.279	0.482	0.207

TABLE 3 | Results of correlation analysis between environmental variables and abundance of *Calanus sinicus* at YSCWM station (3500-09) at night.

Factor	Values of correlation analysis	P-value
Salinity	−0.283	>0.05
Depth	−0.317*	<0.05
DO	0.433*	<0.05
Chla	0.312*	<0.05

* ** indicate significantly higher with $P < 0.05$, respectively.

Our results showed that all of the individuals detected by the VPR remained in the 9°C layers with DO (4–7 mg/L) at 40–70 m. Chl a and DO had a positive relationship, and both were positively correlated with *C. sinicus* abundance. These results suggested that *C. sinicus* may use diel vertical migration to feed at station 3500-09 at night, in addition, avoiding hypoxia may be another purpose but not the main driving factor. Furthermore, field surveys with more stations in different seasons should be conducted in the future to verify the purpose of this strategy.

Over-Summering Hypothesis of *Calanus sinicus*

Wang et al. (2003) focused on the life history strategies of *C. sinicus* in summer, and the majority of *C. sinicus* (C5) remained in the YSCWM. Based on samples collected from different depths, high *C. sinicus* abundance, mainly composed of C5 and female adults, were resident in the bottom layer ($<12^{\circ}\text{C}$) of the YSCWM in summer. *C. sinicus* was found to have a normal DVM in the Yellow Sea but was confined to a certain extent, as the majority of the population ascended to the thermocline but not to the mixed layer at night, and then descended after several hours. Chl a concentration was regarded as the main proxy for potential phytoplankton food of *C. sinicus* in the YSCWM area (Wang et al., 2009). However, simultaneous Chl a produced by the discrete water sampling approach always showed the highest values in mixed surface water above the thermocline with no description of the SCML (Li et al., 2004).

Previous studies proposed that the upper thermal limit of *C. sinicus* might be about 23°C in the field (Uye, 1988) or 27°C after the individuals have acclimated (Zhang et al., 2007). High surface temperature was harmful for breeding, egg hatching and developmental processes. As the *C. sinicus* population could not enter the food-rich hot surface layer (higher than 25°C), researchers presumed that *C. sinicus* had to adopt a confined DVM and use the bottom layer of the YSCWM as a refuge (Zhang et al., 2007). As a result, low temperature and scarce food in the

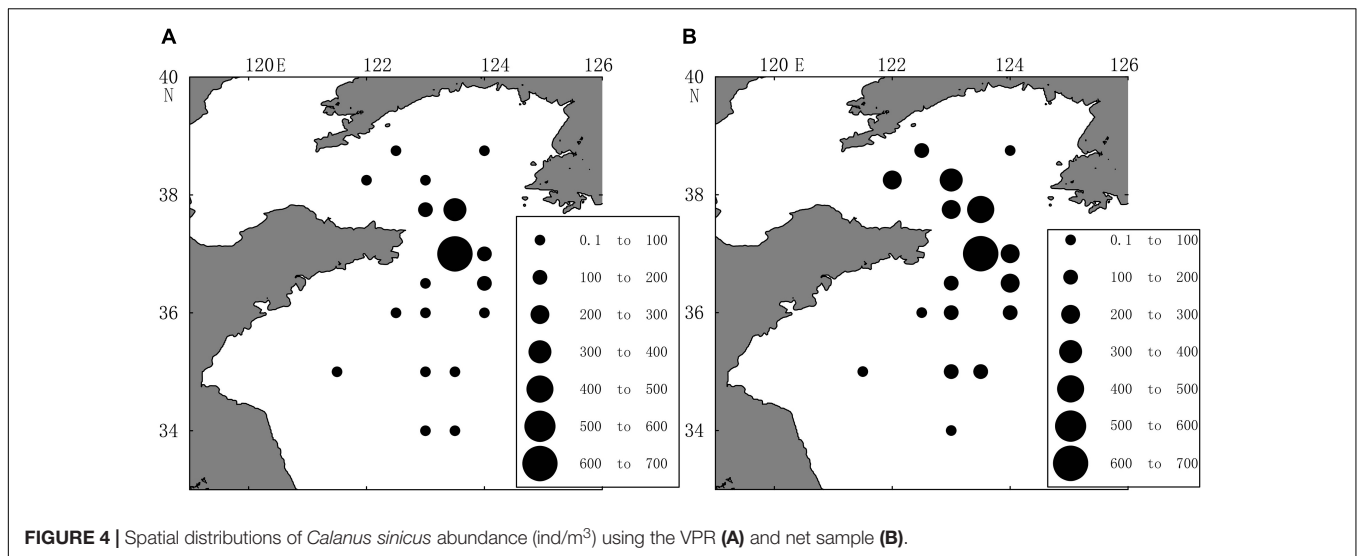


FIGURE 4 | Spatial distributions of *Calanus sinicus* abundance (ind/m³) using the VPR (A) and net sample (B).

YSCWM restrained physiological processes such as reproduction and development of *C. sinicus* (Zhou et al., 2016). Previous studies suggested that clearance of *C. sinicus* in the YSCWM was high on board, but gut pigment contents were relatively low in situ (Li et al., 2004). This situation of low ingestion rates and relatively high oxygen consumption rates induced a net loss of body carbon in *C. sinicus*. Consequently, female individuals could not spawn due to lack of energy, and their oil sac decreased gradually from late spring to early autumn (Sun et al., 2011). Both respiration rate and RNA expression suggested that C5 individuals stopped developing, but were not in diapause (Li et al., 2004; Zhou et al., 2016).

The main observation data in this study were on vertical distribution and analysis. The data collected using the plankton net showed that the range of abundance in the surveyed area was 0–700 ind/m³. Shi et al. (2019) obtained similar results with a range of abundance of 16.9–423.7 ind/m³, and the data on the layered network of the YSCWM has a certain reference significance for analysis. Liu et al. (2003) focused on the frontal area in the Yellow Sea, and the abundance was less than 200 ind/m³ in the frontal zone. The results of Yin et al. (2011) showed the seasonal change, where the spring abundance was $23 \pm (77.78)$ ind/m³ and the summer abundance was $13.74 \pm (45.1)$ ind/m³ in the South China Sea. Previous research showed the results of using a traditional net to collect *C. sinicus* in the whole water layer and average them. While the local high value was not truly reflected, the results of this study better describes the local high value in order to reflect the actual *C. sinicus* vertical distribution using the VPR.

The Yellow Sea Warm Current, a branch of the Tsushima Warm Current originating from the Kuroshio region in the East China Sea, carries warmer and saltier water northward into the Yellow Sea. This current, together with the southward flowing coastal currents, plays an important role in the water exchange within the Yellow Sea (Shi et al., 2019). In winter, zooplankton communities in the Yellow Sea were dominated by temperate and warm-temperate species, such as *C. sinicus* (Chen et al., 2020). However, we have no relevant data at present on advection and

require further data in future. *C. sinicus* inside the YSCWM is probably quiescent in summer (Zhou et al., 2016), their activity and energy supply are insufficient to achieve migration, and we believe that most of the species observed using the VPR are local species.

Vertical Migration and Its Driving Force in *Calanus sinicus*

Investigations into the relationships between vertical distributions of zooplankton and the SCML require fine-scale sampling approaches and datasets on contemporary circumstances. The VPR provided more details on both vertical distribution profiles of *C. sinicus* and simultaneous Chl *a* levels in the YSCWM area in summer (Figure 3). The SCML was only several meters higher than the location of the *C. sinicus* population, which potentially induced DVM. However, only a small portion of *C. sinicus* ascended to the SCML at seven of 18 stations (3600-05, 3650-05, 3775-04, 3775-05, 3825-02, 3825-05, and 3875-02), while the main population of *C. sinicus* remained in the foodless YSCWM regardless of the survey time (Figure 3). Pu et al. (2004) showed that the vertical migration ability of *C. sinicus* was weak and only a few migrated to the thermocline; in general, the vertical distribution of *C. sinicus* revealed the confined range of classical DVM, which was similar to the results of previous studies (Zhang et al., 2007). Kang et al. (2013) observed that the major *C. sinicus* population did not migrate into the surface water even at stations where the surface temperature was comfortable (less than 20°C), indicating that there were other driving forces in addition to surface temperature. Thus, predation was speculated to be the main reason for the confined DVM.

Irrespective of simulated or in situ studies in either fresh water or marine ecosystems, numerous reports proposed that the DVM is a zooplankton behavioral feedback determined by trade-off between growth and evasion of predation risk (Pinti and Visser, 2019). Prey often use cold and dark deep water as a refuge to avoid predation from visual predators, and ascend to feed in the surface water at night (Mehner, 2012; Thygesen and

Patterson, 2019; Moller et al., 2020). Due to the disadvantages of a cold and foodless environment in the deep layer, migrants often reduce their rate of development and reproductive fitness. Due to their energy intake requirements, herbivorous copepods may ascend to ingest food when circumstances are appropriate. Consequently, remaining in the SCML might be an optimal choice for them at night. In the English Channel, the majority of the *C. helgolandicus* population was found to remain in the SCML during the night in summer, where the seawater column was also highly stratified (Harris, 1988). Xu et al. (2016) reported that the sound scattering layer, which was attributed to copepods (mainly *C. sinicus* and *Euchaeta* spp.), migrated upward and remained in the SCML beneath the thermocline at night in the East China Sea. Particles 100–150 μm in size decreased simultaneously in the layer, and were considered to be ingested by copepods (Xu et al., 2016).

Previous studies suggested that predation could induce the descent of marine copepods such as *Acartia hudsonica* and *Pseudodiaptomus* spp. (Frost and Bollens, 2011), and reduce their feeding activation regardless of illumination (Bollens, 1996). The over-wintering strategy of *Calanus* spp., which descend to the deep, cold, and dark domain of the Atlantic Ocean seasonally in a dormant state, was recognized to be partially driven by predation from planktivorous fish (Bagoien et al., 2001). In the Yellow Sea, the *C. sinicus* population suffered significant predation pressure from the anchovy *Engraulis japonicus* (Kang et al., 2013). Predation by sardines and anchovies was thought to be the primary reason affecting the DVM of *C. sinicus* in the Japan inland sea (Uye, 1988). The hot areas of anchovy distribution were mainly located in and at the edge of the YSCWM area in summer (Niu et al., 2013) and *E. japonicus* often aggregated in and above the thermocline layer (Wan et al., 2008). The VPR and probes demonstrated confined vertical migration of *C. sinicus* in the Yellow Sea in the present study, although the distribution of the SCML was suitable. Therefore, avoidance of predators was presumed to be the most probable driving force regulating the DVM of *C. sinicus* in the Yellow Sea in summer. The simultaneous diel vertical distributions of Chl a, copepod *C. sinicus* and anchovy *E. japonicus* should be further studied.

Lipid accumulation is deemed to be an important factor affecting the DVM of copepods. In the Arctic Ocean, *Calanus* spp. with a high lipid load were found to remain in the deep water, while individuals with a lower lipid load and all *Metridia longa* developmental stages continued normal DVM. Substantial lipid reserves of *Calanus* spp. are considered to be the main energy resource after diapause, while *M. longa* adopted a combined strategy of active feeding and lipid accumulation to overcome the Arctic conditions in winter (Schmid et al., 2018). The average value of the relative oil sac volume (expressed as % of body volume) of *C. sinicus* (about 30–35%) in the YSCWM (Sun et al., 2011) was lower than that of *Calanus* spp. (about 50–80%) in the Arctic Ocean (Schmid et al., 2018). In addition, part of the *C. sinicus* population developed and the oil sac shrank gradually during summer (Wang et al., 2009) and evidence from the grazing impact of *C. sinicus* (Li et al., 2004), oxygen consumption rate and gene expression (Zhou et al., 2016), all support that the over-summering strategy of *C. sinicus* in the YSCWM is quiescent and not diapause, which is similar to the combined strategy of

M. longa. Therefore, lipid accumulation may not be the factor that ceases DVM of *C. sinicus*. The detailed relationships between lipid fullness and DVM of *C. sinicus* remain to be explored in future studies.

CONCLUSION

In this study, the VPR was used to determine the refined vertical distribution characteristics of *Calanus sinicus* in the Yellow Sea. Environmental factors affecting the vertical distribution of *C. sinicus* are discussed and statistically analyzed in this study. The influence of the SCML on *C. sinicus* vertical distribution has seldom been described. The relationship between abundance and Chl a, showed that the diel vertical migration trend in *C. sinicus* is to feed at night in the YSCWM. In addition to temperature, DO concentrations, and the column depth are also influencing factors.

DATA AVAILABILITY STATEMENT

The datasets generated for this study are available on request to the corresponding author.

AUTHOR CONTRIBUTIONS

JP, FC, FY, and YS contributed to the conception of the study. JP, XD, CW, and FS contributed to sample collection and data collation. JP, GS, FS, and YZ analyzed the samples and conducted the data analyses. JP, FC, and YS wrote the manuscript and contributed to the definition of aims. All authors contributed to improvement of the manuscript before approving it for submission.

FUNDING

This study was supported by the National Natural Science Foundation of China (Grant Nos. 41806164 and 41349902), Strategic Priority Research Program of the Chinese Academy of Sciences (Grant Nos. XDA11020301 and XDA11020305), the Natural Science Foundation of Shandong Province (Grant No. ZR2020QD104), and International Science Partnership Program of the Chinese Academy of Sciences (Grant No. 133137KYSB20200002).

ACKNOWLEDGMENTS

The authors warmly thank Guangtao Zhang, Xiaoxia Sun, Qiang Ren, Zheng Li, Hang Yin, Shujin Guo, the Research Vessel Operation and Management Center, and the Jiaozhou Bay Marine Ecosystem Research Station for their continuous support on board. Our deepest gratitude goes to the reviewers and editors for their careful work and thoughtful suggestions that have helped improve this paper substantially.

REFERENCES

- Ashjian, C. J., Davis, C. S., Gallagher, S. M., and Alatalo, P. (2001). Distribution of plankton, particles, and hydrographic features across georges bank described using the video plankton recorder. *Deep Sea Res. Part II Top. Stud. Oceanogr.* 48, 245–282.
- Bagoien, E., Kaartvedt, S., Aksnes, D. L., and Eiane, K. (2001). Vertical distribution and mortality of overwintering *Calanus*. *Limnol. Oceanogr.* 46, 1494–1510. doi: 10.4319/lo.2001.46.6.1494
- Benfield, M. C., Davis, C. S., Wiebe, P. H., Gallagher, S. M., Lough, R. G., and Copley, N. J. (1996). Video plankton recorder estimates of copepod, pteropod and larvacean distributions from a stratified region of georges bank with comparative measurements from a MOCNESS sampler. *Deep-Sea Res. Part II Top. Stud. Oceanogr.* 43, 1925–1945. doi: 10.1016/s0967-0645(96)00044-6
- Bo, L. H., Tian, X., Tao, D., and Hua, L. R. (2006). The distribution of bacterioplankton in the yellow sea cold water mass (YSCWM). *Acta Ecol. Sin.* 26, 1012–1019. doi: 10.1016/s1872-2032(06)60020-6
- Bollens, S. M. (1996). Diel vertical migration in zooplankton: trade-offs between predators and food. *Oceanus* v39, 1359–1365. doi: 10.1093/plankt/13.6.1359
- Broughton, E. A., and Lough, R. G. (2006). A direct comparison of MOCNESS and video plankton recorder zooplankton abundance estimates: possible applications for augmenting net sampling with video systems. *Deep Sea Res. Part II* 53, 2789–2807. doi: 10.1016/j.dsr2.2006.08.013
- Chen, H., Zhu, Y., and Liu, G. (2020). Characteristics of zooplankton community in north yellow sea unveiled an indicator species for the yellow sea warm current in winter: *Euchaeta plana*. *J. Oceanol. Limnol.* 38, 1762–1770. doi: 10.1007/s00343-019-9165-y
- Chen, Q. (1964). A study of the breeding periods, variation in sex ratio and in size of *Calanus sinicus* Brodsky. *Oceanol. Limnol. Sin.* 6, 272–288.
- Davis, C. S., Gallagher, S. M., and Solow, A. R. (1992). Microaggregations of oceanic plankton observed by towed video microscopy. *Science* 257:230.
- Davis, C. S., Thwaites, F. T., Gallagher, S. M., and Hu, Q. (2005). A three-axis fast-tow digital video plankton recorder for rapid surveys of plankton taxa and hydrography. *Limnol. Oceanogr. Methods* 3, 59–74. doi: 10.4319/lom.2005.3.59
- Everett, J. D., Baird, M. E., Buchanan, P., Bulman, C., Davies, C., Downie, R., et al. (2017). Modeling what we sample and sampling what we model: challenges for zooplankton model assessment. *Front. Mar. Sci* 4:77. doi: 10.3389/fmars.2017.00077
- Fei, Y., Zhixi, Z., Diao, X., Jingsong, G., and Yuxiang, T. (2006). Analysis of evolution of the Huanghai Sea cold water mass and its relationship with adjacent water masses. *Acta Oceanol. Sin.* 28, 26–34.
- Frost, B. W., and Bollens, S. M. (2011). Variability of diel vertical migration in the marine planktonic Copepod *Pseudocalanus newmani* in relation to its predators. *Can. J. Fish. Aquat. Sci.* 49, 1137–1141. doi: 10.1139/f92-126
- Fu, M., Wang, Z., Li, Y., Li, R., Sun, P., Wei, X., et al. (2009). Phytoplankton biomass size structure and its regulation in the southern yellow sea (China): seasonal variability. *Cont. Shelf Res.* 29, 2178–2194.
- Gislason, A., Kai, L., and Martensdotter, G. (2016). The cross-shore distribution of plankton and particles southwest of Iceland observed with a video plankton recorder. *Cont. Shelf Res.* 123, 50–60.
- Gong, X., Jiang, W., Wang, L., Gao, H., Boss, E., Yao, X., et al. (2017). Analytical solution of the nitracline with the evolution of subsurface chlorophyll maximum in stratified water columns. *Biogeosciences* 14, 2371–2386. doi: 10.5194/bg-14-2371-2017
- Harris, R. P. (1988). Interactions between diel vertical migratory behavior of marine zooplankton and the subsurface chlorophyll maximum. *Bull. Mar. Sci.* 43, 663–674.
- Hu, Q., and Davis, C. (2006). Accurate automatic quantification of taxa-specific plankton abundance using dual classification with correction. *Mar. Ecol. Prog. Ser.* 306, 51–61. doi: 10.3354/meps306051
- Huo, Y., Sun, S., Zhang, F., Wang, M., Li, C., and Yang, B. (2012). Biomass and estimated production properties of size-fractionated zooplankton in the yellow sea, China. *J. Mar. Syst.* 94, 1–8. doi: 10.1016/j.jmarsys.2011.09.013
- Hwang, J.-S., and Wong, C. K. (2005). The china coastal current as a driving force for transporting *Calanus sinicus* (Copepoda: Calanoida) from its population centers to waters off Taiwan and Hong Kong during the winter northeast monsoon period. *J. Plankton Res.* 27, 205–210. doi: 10.1093/plankt/fbh162
- Jónasdóttir, S. H. (2010). Lipid content of *Calanus finmarchicus* during overwintering in the Faroe-Shetland Channel. *Fish. Oceanogr.* 8, 61–72. doi: 10.1046/j.1365-2419.1999.00003.x
- Kang, J.-H., Seo, M., Kwon, O. Y., and Kim, W.-S. (2013). Diel vertical migration of the copepod *Calanus sinicus* before and during formation of the yellow sea cold bottom water in the yellow sea. *Acta Oceanol. Sin.* 32, 99–106. doi: 10.1007/s13131-013-0357-6
- Kim, G., and Kang, H.-K. (2018). Grazing impact of the copepod *Calanus sinicus* on phytoplankton in the Northern East China Sea in late spring. *Ocean Sci. J.* 53, 225–237. doi: 10.1007/s12601-018-0010-6
- Li, C., Sun, S., Wang, R., and Wang, X. (2004). Feeding and respiration rates of a planktonic copepod (*Calanus sinicus*) overwintering in yellow sea cold bottom waters. *Mar. Biol.* 145, 149–157.
- Li, K., Yan, Y., Yin, J., Tan, Y., and Huang, L. (2016). Seasonal occurrence of *Calanus sinicus* in the northern South China Sea: a case study in Daya Bay. *J. Mar. Syst.* 159, 132–141. doi: 10.1016/j.jmarsys.2016.03.014
- Li, Z., Zhang, X. L., Wang, Z. L., Sun, P., and Zong-Jun, X. U. (2011). Preliminary study on vertical distribution pattern of chlorophyll a in south yellow sea in summer 2008 (in Chinese with English abstract). *Adv. Mar. Sci.* 29, 81–89.
- Liu, G. M., Sun S., Wang, H., Zhand, Y., Yang, B., and Ji, P. (2003). Abundance of *Calanus sinicus* across the tidal front in the Yellow Sea, China. *Fisheries Oceanography* 12, 291–298. doi: 10.1046/j.1365-2419.2003.00253.x
- Mehner, T. (2012). Diel vertical migration of freshwater fishes - proximate triggers, ultimate causes and research perspectives. *Freshw. Biol.* 57, 1342–1359. doi: 10.1111/j.1365-2427.2012.02811.x
- Moller, K. O., St John, M., Temming, A., Diekmann, R., Peters, J., Floeter, J., et al. (2020). Predation risk triggers copepod small-scale behavior in the Baltic Sea. *J. Plankton Res.* 42, 702–713.
- Niu, M., Wang, J., Yuan, W., Zhu, J., and Dai, F. (2013). Seasonal dissimilarity of *Engraulis japonicus* spatiotemporal distribution in yellow sea. *Chin. J. Ecol.* 32, 114–120.
- Norrbin, F., Eilertsen, H. C., and Degerlund, M. (2009). Vertical distribution of primary producers and zooplankton grazers during different phases of the Arctic spring bloom. *Deep Sea Res. Part II* 56, 1945–1958. doi: 10.1016/j.dsr2.2008.11.006
- Pan, J., Cheng, F., and Yu, F. (2018). The diel vertical migration of zooplankton in the hypoxia area observed by video plankton recorder. *Indian J. Geo Mar. Sci.* 47, 1353–1363.
- Park, S., Chu, P. C., and Lee, J. H. (2011). Interannual-to-interdecadal variability of the yellow sea cold water mass in 1967–2008: characteristics and seasonal forcings. *J. Mar. Syst.* 87, 177–193.
- Pinti, J., and Visser, A. W. (2019). Predator-prey games in multiple habitats reveal mixed strategies in diel vertical migration. *Am. Nat.* 193, E65–E77. doi: 10.1086/701041
- Pu, X. M., Sun, S., Yang, B., Zhang, G. T., and Zhang, F. (2004). Life history strategies of *Calanus sinicus* in the southern yellow sea in summer. *J. Plankton Res.* 26, 1059–1068. doi: 10.1093/plankt/fbh101
- Ross, T. (2014). A video-plankton and microstructure profiler for the exploration of in situ connections between zooplankton and turbulence. *Deep Sea Res. Part I* 89, 1–10.
- Sainmont, J., Gislason, A., Heuschele, J., Webster, C. N., Sylvander, P., Wang, M., et al. (2014). Inter- and intra-specific diurnal habitat selection of zooplankton during the spring bloom observed by video plankton recorder. *Mar. Biol.* 161, 1931–1941. doi: 10.1007/s00227-014-2475-x
- Schlitzer, R. (2002). Interactive analysis and visualization of geoscience data with ocean data view. *Comput. Geosci.* 28, 1211–1218.
- Schmid, M. S., Maps, F., and Fortier, L. (2018). Lipid load triggers migration to diapause in Arctic *Calanus* copepods—insights from underwater imaging. *J. Plankton Res.* 40, 311–325. doi: 10.1093/plankt/fby012
- Shi, Y., Sun, S., Li, C., Zhang, G., Yang, B., and Ji, P. (2019). Changes in the population structure of *Calanus sinicus* during summer-autumn in the southern yellow sea. *Acta Oceanol. Sin.* 38, 56–63. doi: 10.1007/s13131-019-1435-1
- Stanley, R. H. R., Mcgillicuddy, D. J., Sandwith, Z. O., and Pleskow, H. M. (2017). Submesoscale hotspots of productivity and respiration: insights from high-resolution oxygen and fluorescence sections. *Deep Sea Res. Part I Oceanogr. Res. Papers* 130, 1–11.
- Su, N., Du, J., Liu, S., and Zhang, J. (2013). Nutrient fluxes via radium isotopes from the coast to offshore and from the seafloor to upper waters after the

- 2009 spring bloom in the Yellow Sea. *Deep Sea Res. Part II* 97, 33–42. doi: 10.1016/j.dsr2.2013.05.003
- Sun, S., Huo, Y., and Yang, B. (2010). Zooplankton functional groups on the continental shelf of the yellow sea. *Deep Sea Res. Part II Top. Stud. Oceanogr.* 57, 1006–1016. doi: 10.1016/j.dsr2.2010.02.002
- Sun, S., Li, C., Cheng, F., et al. (2016). *Atlas of Common Zooplankton of Chinese Coastal Seas*. Beijing: Ocean Press.
- Sun, S., Wang, S., and Li, C. (2011). Preliminary study on the oil storage of *Calanus sinicus* fifth copepodites(c5) in the Yellow Sea. *Oceanol. Limnol. Sin.* 42, 165–169.
- Sun, X., Sun, X., Zhu, L., Li, X., and Sun, S. (2020). Seasonal and spatial variation in abundance of the copepod *Calanus sinicus*: effects of decreasing dissolved oxygen and small jellyfish bloom in northern Yellow Sea, China, nearshore waters. *Mar. Pollut. Bull.* 161(Pt B):111653. doi: 10.1016/j.marpolbul.2020.111653
- Takahashi, K., Ichikawa, T., and Tadokoro, K. (2015). Diel colour changes in male *Sapphirina nigromaculata* (Cyclopoida, Copepoda). *J. Plankton Res.* 37:fbv088. doi: 10.1093/plankt/fbv088
- Thygesen, U. H., and Patterson, T. A. (2019). Oceanic diel vertical migrations arising from a predator-prey game. *Theor. Ecol.* 12, 17–29. doi: 10.1007/s12080-018-0385-0
- Uye, S. (1988). Temperature-dependent development and growth of *Calanus sinicus* (Copepoda: Calanoida) in the laboratory. *Hydrobiologia* 167, 285–293. doi: 10.1007/978-94-009-3103-9_28
- Uye, S. (2000). Why does *Calanus sinicus* prosper in the shelf ecosystem of the Northwest Pacific Ocean? *ICES J. Mar. Sci.* 57, 1850–1855.
- Wan, R., Wei, H., Sun, S., and Zhao, X. Y. (2008). Spawning ecology of the anchovy *Engraulis japonicus* in the spawning ground of the Southern Shandong Peninsula I. Abundance and distribution characters of anchovy eggs and larvae. *Acta Zool. Sin.* 54, 785–797.
- Wang, Q. N., Yan, T., and Zhou, M. J. (2013). The effects of hypoxia on survival and reproduction of *Calanus sinicus*. *Mar. Sci.* 37, 12–16.
- Wang, R., Zuo, T., and Wang, K. (2003). The Yellow Sea cold bottom water—an oversummering site for *Calanus sinicus* (Copepoda, Crustacea). *J. Plankton Res.* 25, 169–183.
- Wang, S., Li, C., Sun, S., Ning, X., and Zhang, W. (2009). Spring and autumn reproduction of *Calanus sinicus* in the yellow sea. *Mar. Ecol. Prog. Ser.* 379, 123–133.
- Wang, Y., Li, C., Liu, M., and Jin, X. (2017). Lipids and fatty acids in *Calanus sinicus* during over-summering in the southern yellow sea. *Chin. J. Oceanol. Limnol.* 35, 874–882. doi: 10.1007/s00343-017-5351-y
- Wei, Q.-S., Yu, Z.-G., Wang, B.-D., Fu, M.-Z., Xia, C.-S., Liu, L., et al. (2016). Coupling of the spatial-temporal distributions of nutrients and physical conditions in the southern yellow sea. *J. Mar. Syst.* 156, 30–45. doi: 10.1016/j.jmarsys.2015.12.001
- Xia, C., Qiao, F., Yang, Y., Ma, J., and Yuan, Y. (2006). Three dimensional structure of the summertime circulation in the yellow sea from a wave tide circulation coupled model. *J. Geophys. Res. Oceans* 111:C11S03.
- Xu, J., Xu, Z., and Gao, Q. (2016). Distribution of dominant zooplankton species along a latitudinal gradient in China sea during spring. *J. Ocean Univ. China* 15, 502–508. doi: 10.1007/s11802-016-2871-6
- Yin, J., Huang, L., Li, K., Lian, S., Li, C., and Lin, Q. (2011). Abundance distribution and seasonal variations of *Calanus sinicus* (Copepoda: Calanoida) in the northwest continental shelf of south China Sea. *Cont. Shelf Res.* 31, 1447–1456.
- Zhang, G. T., Sun, S., and Yang, B. (2007). Summer reproduction of the planktonic copepod *Calanus sinicus* in the yellow sea: influences of high surface temperature and cold bottom water. *J. Plankton Res.* 29, 179–186. doi: 10.1093/plankt/fbm005
- Zhang, G.-T., Sun, S., and Zhang, F. (2005). Seasonal variation of reproduction rates and body size of *Calanus sinicus* in the southern yellow sea. *China. J. Plankton Res.* 27, 135–143. doi: 10.1093/plankt/fbh164
- Zhou, K., and Sun, S. (2016). Effect of diurnal temperature difference on lipid accumulation and development in *Calanus sinicus* (Copepoda: Calanoida). *Chin. J. Oceanol. Limnol.* 35, 745–753. doi: 10.1007/s00343-017-6039-z
- Zhou, K., Sun, S., Wang, M., Wang, S., and Li, C. (2016). Differences in the physiological processes of *Calanus sinicus* inside and outside the Yellow Sea Cold Water Mass. *Journal of Plankton Research* 38, 551–563. doi: 10.1093/plankt/fbw011

Conflict of Interest: The authors declare that the research was conducted in the absence of any commercial or financial relationships that could be construed as a potential conflict of interest.

Publisher's Note: All claims expressed in this article are solely those of the authors and do not necessarily represent those of their affiliated organizations, or those of the publisher, the editors and the reviewers. Any product that may be evaluated in this article, or claim that may be made by its manufacturer, is not guaranteed or endorsed by the publisher.

Copyright © 2021 Pan, Cheng, Yu, Shi, Sun, Si, Wei, Diao and Zhao. This is an open-access article distributed under the terms of the Creative Commons Attribution License (CC BY). The use, distribution or reproduction in other forums is permitted, provided the original author(s) and the copyright owner(s) are credited and that the original publication in this journal is cited, in accordance with accepted academic practice. No use, distribution or reproduction is permitted which does not comply with these terms.